Electronic Supplementary Information for

A multiphase Pd metallene doped with Cu atoms for promoting the electrocatalytic oxidation performance of ethanol

Hui Wang,[a] Xiang Li,[a]* Zitong Jiang,[a] Qing Xu,[a] Tao Zhang,[a] Qinghua Zuo,[a] Chenbo wang,[a] Qiaoqin Guo[a]

[a]Shaanxi Key Laboratory of Optoelectronic Functional Materials and Devices, School of Materials Science and Chemical Engineering, Xi'an Technological University, Xi'an, Shaanxi 710021, China

*To whom correspondence should be addressed. E-mail: lixiang@xatu.edu.cn.

Experimental

Materials

Palladium (II) 2, 4-pentanedionate ($Pd(acac)_2$,34.7%) was purchased from Innochem. Commercial Pd/C (10 wt %) was ordered from Innochem. Nafion solution (5 wt%) was purchased from Macklin. Copper acetylacetonate ($Cu(acac)_2$, 97%), Molybdenum hexacarbonyl ($Mo(CO)_6$, 99.9%), Acetic acid glacial (CH_3COOH, 99.5%), N, N-Dimethylformamide (DMF, 99.5%), Ethanol (99.7%) and potassium hydroxide (85%) were purchased from Aladdin.

Synthesis of the pure Pd metallene nanocatalyst

Place 10 mg of $Pd(acac)_2$, 30 mg of $Mo(CO)_6$, and 10 mL of N,N-dimethylformamide (DMF) into a 30 mL glass bottle. Subject the mixture to ultrasonic agitation for 10 minutes until it becomes thoroughly homogeneous. Subsequently, introduce 5 mL of acetic acid. After ensuring uniform sonication, transfer the bottle to a 60 °C oil bath and maintain continuous heating for 6 hours. Once the reaction is complete, remove the glass bottle and let it cool down to room temperature. Centrifuge the mixture at a speed of 6000 rpm for 3 minutes, rinse it three times with ethanol, and finally, disperse the Pd metallene in ethanol for future use.

Synthesis of Cu-doped Pd-based metallene nanocatalyst

Prepare four 30 mL glass bottles. Add 10 mg of $Pd(acac)_2$ and 30 mg of $Mo(CO)_6$ to each bottle. Then, sequentially add 2 mg, 4 mg, 6 mg, and 8 mg of $Cu(acac)_2$ to the respective bottles. Afterward, pour 10 mL of N,N-dimethylformamide (DMF) into each bottle. Subject the mixtures to ultrasonic agitation for 10 minutes until they are completely homogeneous. Next, add 5 mL of acetic acid to each bottle. After achieving uniform sonication, place the bottles in a 60 °C oil bath and keep them heated continuously for 6 hours. Once the reactions are finished, remove the glass bottles and allow them to cool to room temperature. Centrifuge the mixtures at a speed of 6000 rpm for 3 minutes. Rinse them three times with ethanol under identical conditions. Finally, disperse the PdCu metallene in ethanol for subsequent use.

Preparation of the working electrodes

The electrochemical tests in this thesis were conducted within a standard three-electrode system. All electrochemical measurements were carried out using an

electrochemical workstation (CHI660E, Electrochemical Analyzer). A Hg/HgO electrode was employed as the reference electrode, and a platinum (Pt) mesh served as the counter electrode. Subsequently, 20 μL of the catalyst ink was dropped onto a glassy carbon rotating disk electrode (with an area of 0.196 cm^2). This was done in such a way that the weight of the Cu-atom-doped Pd-based metallene nanocatalyst amounted to 6 μg. After allowing it to air-dry naturally, the working electrode was immersed into the electrolyte solution. Then, the reference electrode and the counter electrode were properly connected.

Electrochemical measurements

Cyclic voltammetry (CV) curves were measured at a scan rate of 50 mV/s in a 1.0 M KOH solution. The electrochemical active surface area (ECSA) was calculated via the CO-stripping. For the ethanol oxidation tests, CV curves of the catalyst were recorded at a scan rate of 50 mV/s within a potential range of 0.05 to 1.2 V (vs. RHE) in electrolytes of either 1.0 M KOH or 1.0 M KOH + 1.0 M CH_3CH_2OH. Regarding the stability tests, chronoamperometry (i-t) measurements were adopted. The reaction was carried out for 3600 s at a constant potential of 0.72 V in an electrolyte consisting of 1.0 M KOH + 1.0 M CH_3CH_2OH. All the potentials mentioned in this paper were converted to the reversible hydrogen electrode (RHE) scale. In the context of ethanol oxidation, the catalytic activity for ethanol oxidation in the Cu-atom-doped Pd-based metallene nanocatalyst was determined by normalizing the measured maximum oxidation peak current density with respect to the mass of Pd used and the active surface area.

Characterizations

Transmission electron microscopy (TEM) characterizations were conducted using a JEOL JEM-F200 instrument. Powder X-ray diffraction (XRD) patterns were recorded with a D2 PHASER Gen2 system from Bruker. Inductively coupled plasma mass spectrometry (ICP-MS) analyses were performed on an Agilent 7800 platform. X-ray photoelectron spectroscopy (XPS) measurements were carried out using a Shimadzu/Kratos AXIS SUPRA+ system. Atomic force microscopy (AFM) images were acquired with a Bruker Dimension Icon microscope.

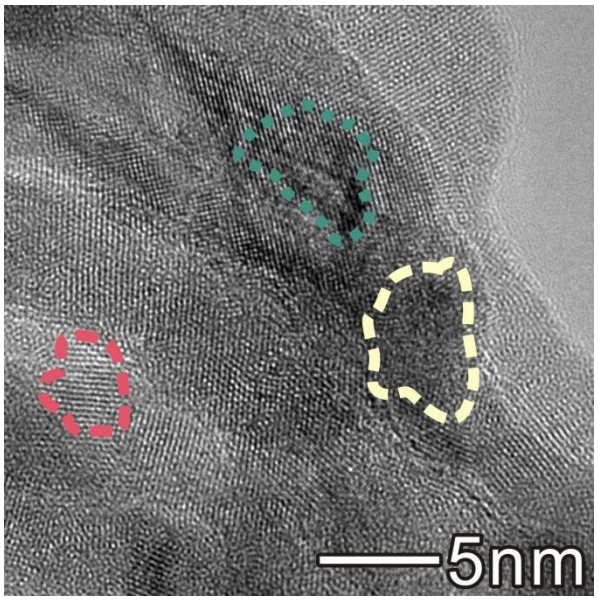

Figure S1. The magnified HRTEM image of the $PdCu_{0.135}$ metallene.

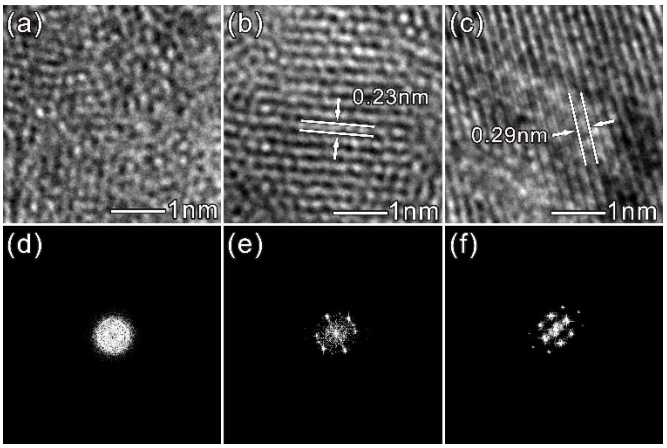

Figure S2. (a-c) The enlarged HRTEM images corresponding to regions highlighted in Figure e, and (d-f) the corresponding FFT patterns of (a)-(c).

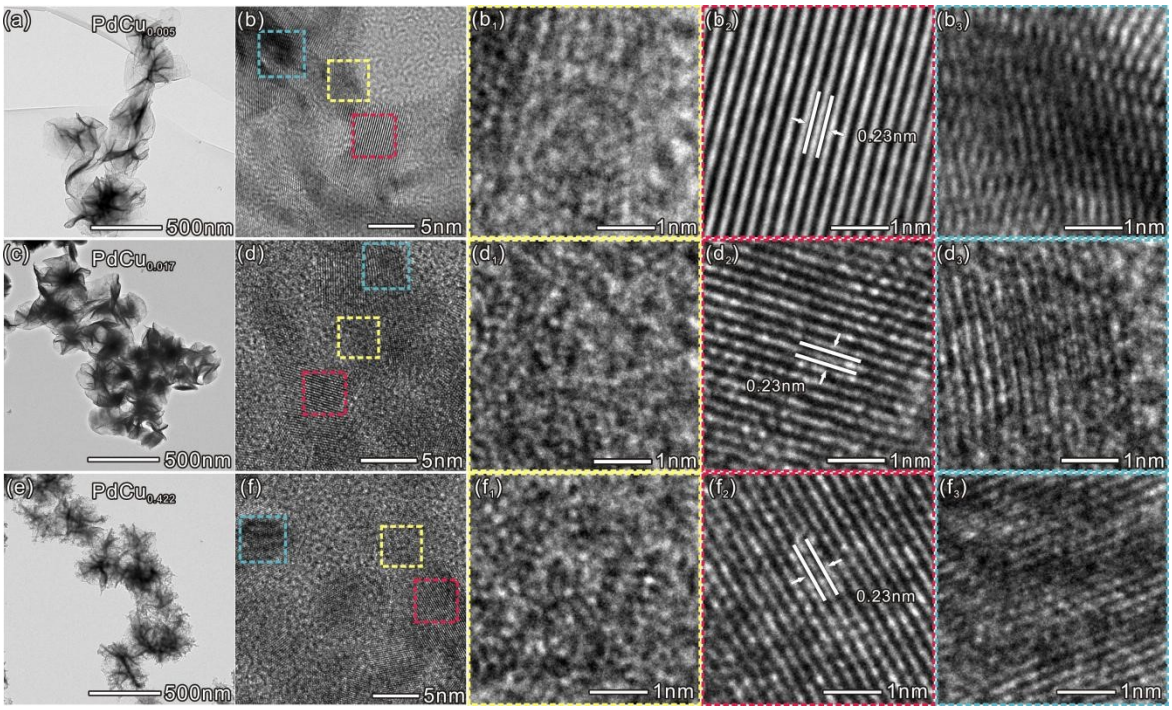

Figure S3. The TEM characterizations of the different compositions of PdCu metallene nanocatalysts. (a, c, e) TEM images. (b, d, f) HRTEM images. (b_1, d_1, f_1) Amorphous structure. (b_2, d_2, f_2) Crystalline structure. (b_3, d_3, f_3) Intermetallic structure.

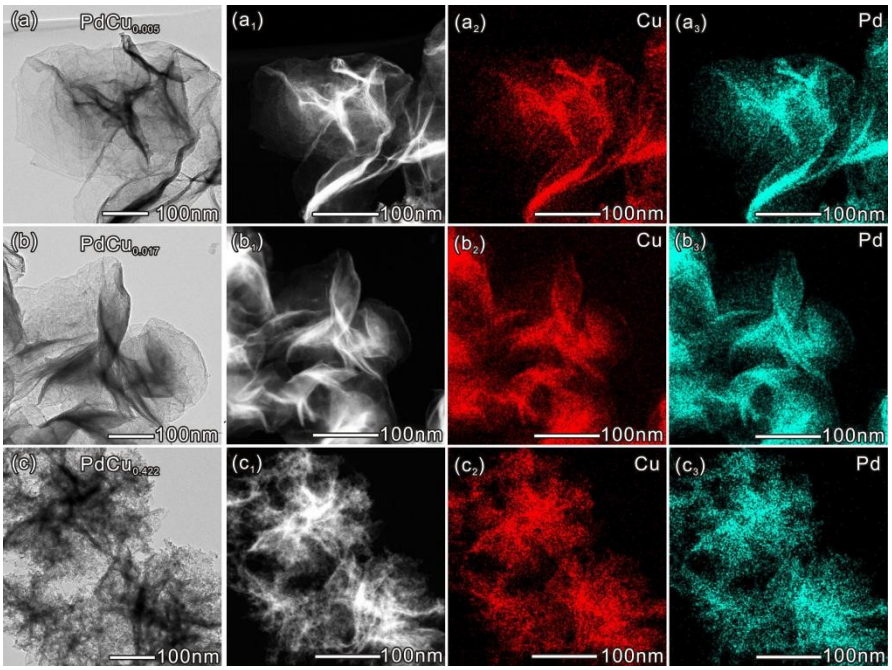

Figure S4. The Characterizations of PdCu metallene nanocatalysts. (a-c) TEM images. (a_1-c_1) HAADF-STEM images. (a_2-c_2, a_3-c_3) EDX elemental mapping images.

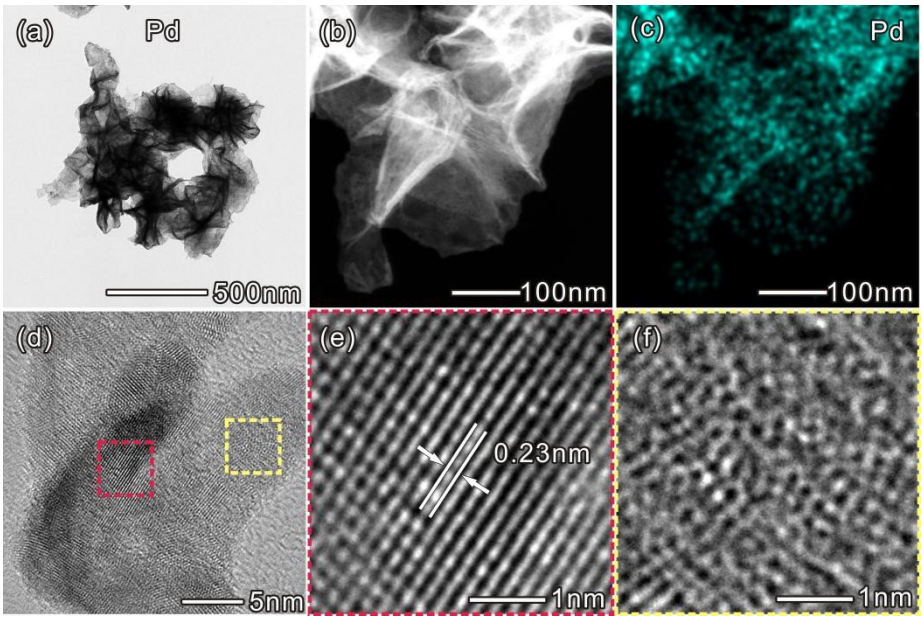

Figure S5. The TEM characterization of Pd metallene nanocatalyst. (a) TEM image. (b) HAADF-STEM image. (c) EDX mapping image. (d) HRTEM image. (e) Crystalline structure. (f) Amorphous structure.

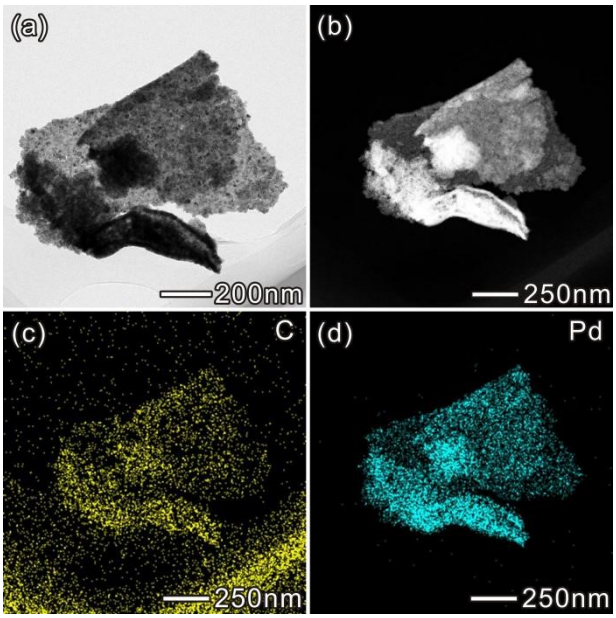

Figure S6. The structural characterization of commercial Pd/C catayst. (a) TEM image. (b) HAAD-STEM image. (c, d) EDX elemental mapping images.

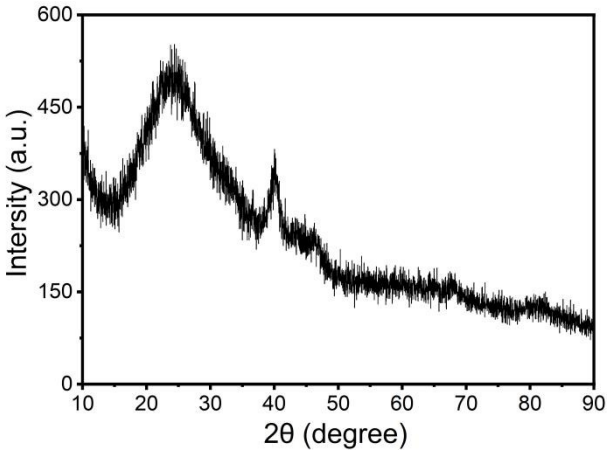

Figure S7. The XRD pattern of the commercial Pd/C catayst.

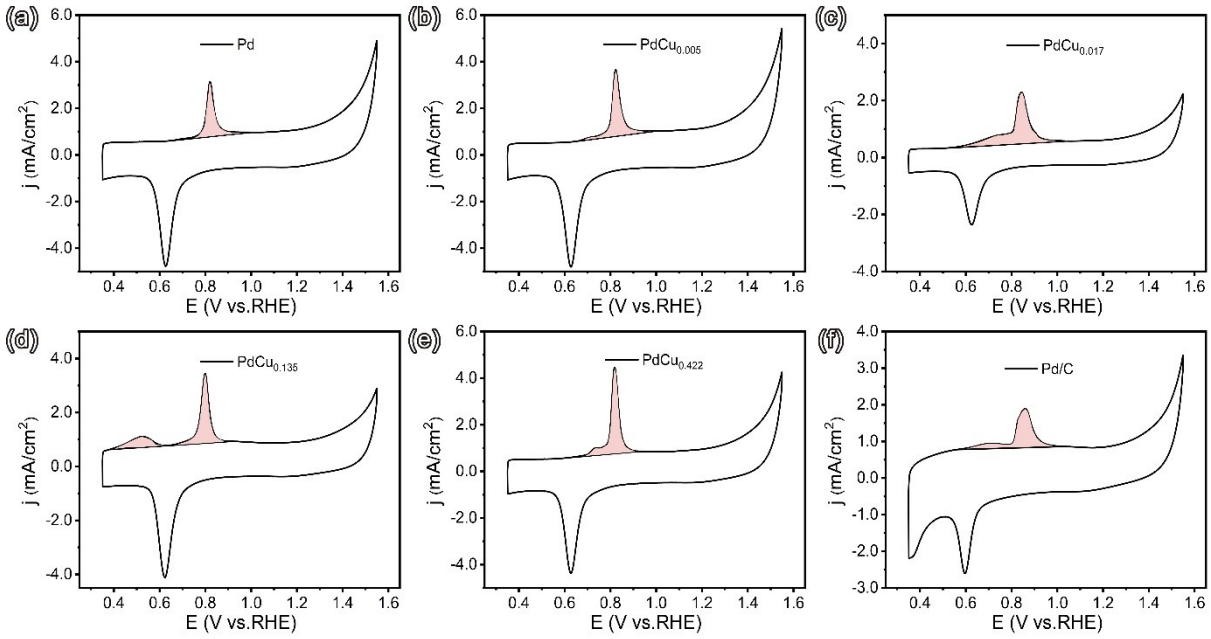

Figure S8. Cyclic voltammetry curves of the different compositions of PdCu metallene nanocatalyst, undoped Pd metallene nanocatalyst, and commercial Pd/C catalyst in CO-saturated KOH (1 M) solution at a scanning rate of 50 mV/s.

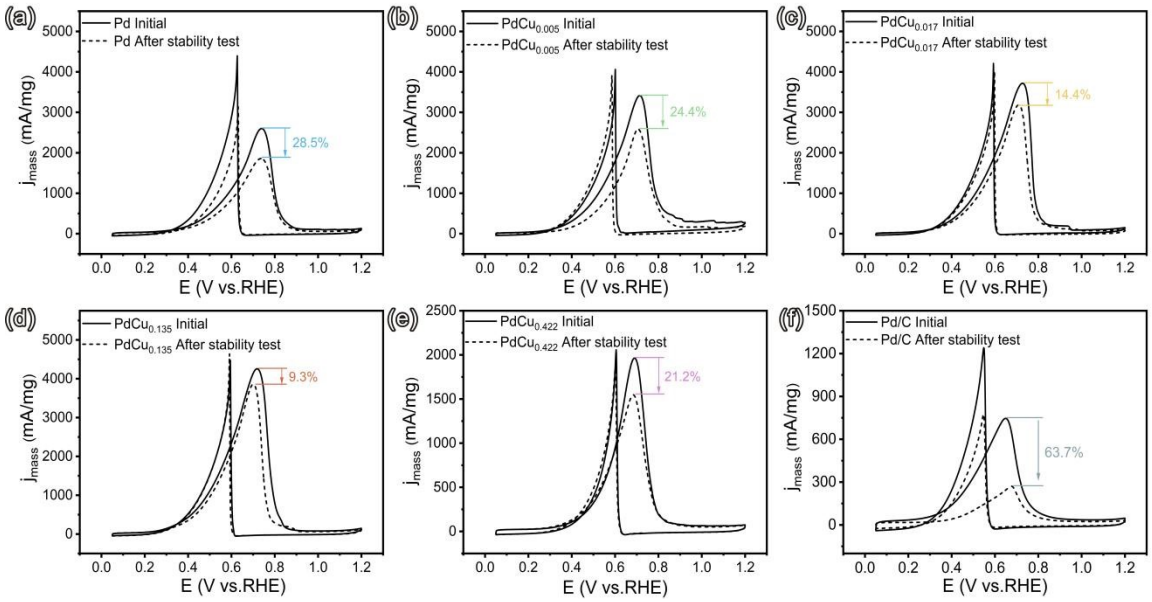

Figure S9. Cyclic voltammetry curves of the different compositions of PdCu metallene nanocatalyst, undoped Pd metallene nanocatalyst, and commercial Pd/C catalyst in N_2-saturated CH_3CH_2OH (1 M) + KOH (1 M) solution at a scanning rate of 50 mV/s before and after the stability testing.

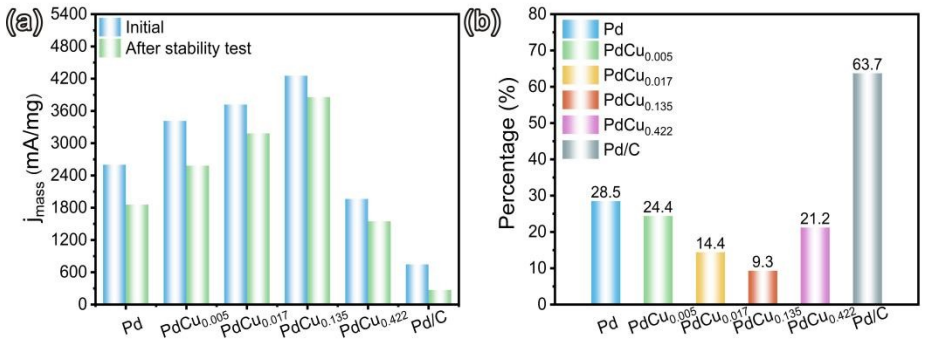

Figure S10. The EOR stability performances of the different compositions of PdCu metallene nanocatalyst, undoped Pd metallene nanocatalyst, and commercial Pd/C catalyst before and after durability testing. (a) Mass activities. (b) The loss percentage of current density.

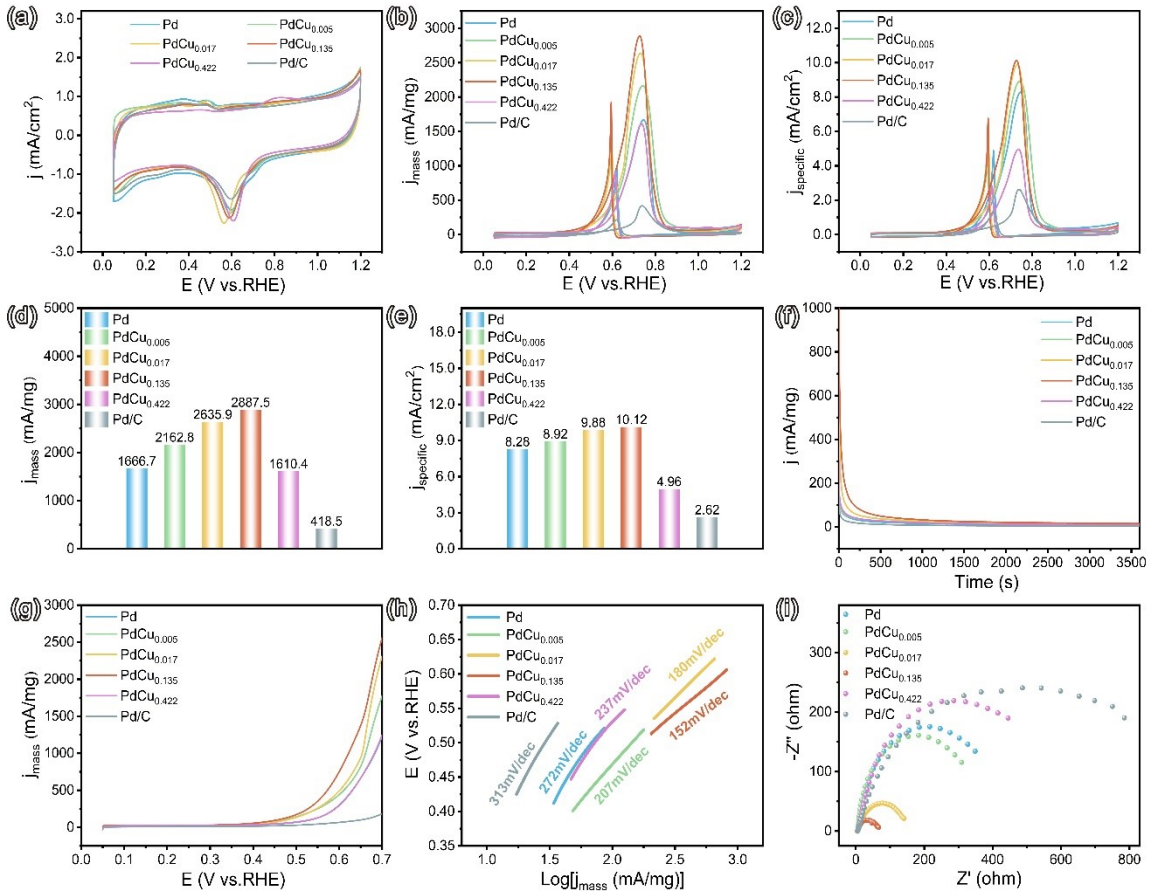

Figure S11. The MeOR performances of the different compositions of PdCu metallene nanocatalyst, undoped Pd metallene nanocatalyst, and commercial Pd/C catalyst. (a) Cyclic voltammetry curves in N_2-saturated KOH (1 M) solution. (b, c) Cyclic voltammetry curves in N_2-saturated CH_3OH (1 M) + KOH (1 M) solution. (d) Mass (j_{mass}) and (e) specific ($j_{specific}$) activities, the values obtained at the peak current. (f) Chronoamperometry curves of the catalysts at 0.75 V current in N_2-saturated CH_3OH (1 M) + KOH (1 M) solution. (g) Onset potential curves. (h) Tafel slope curves. (i) EIS nyquist plots recorded in KOH (1 M) solution.

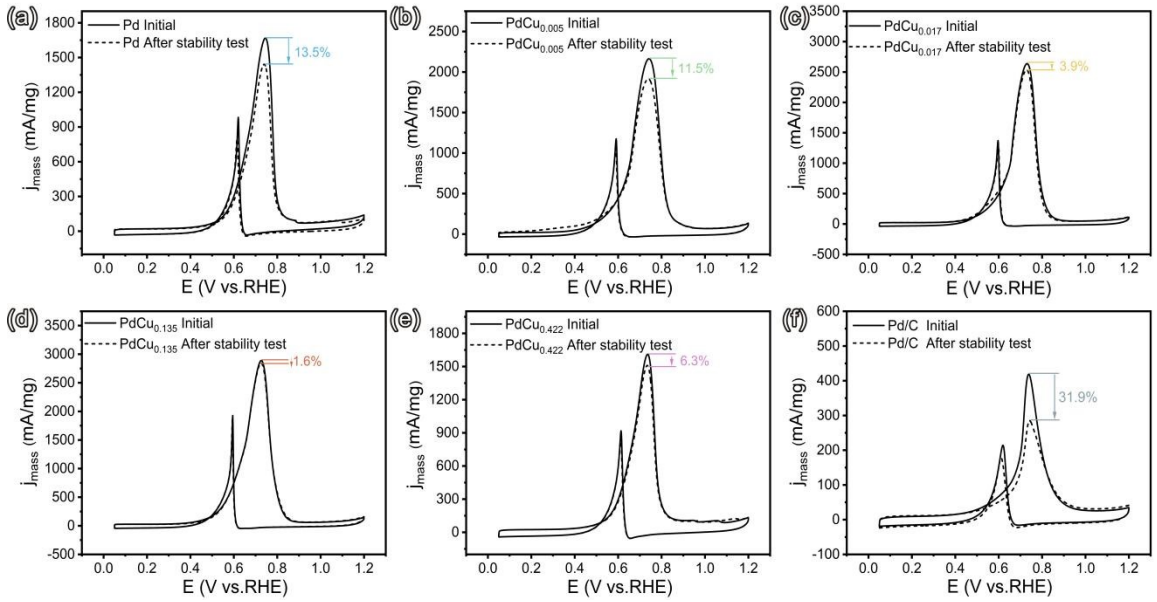

Figure S12. Cyclic voltammetry curves of the different compositions of PdCu metallene nanocatalyst, undoped Pd metallene nanocatalyst, and commercial Pd/C catalyst in N_2-saturated CH_3OH (1 M) + KOH (1 M) solution at a scanning rate of 50 mV/s before and after the stability testing.

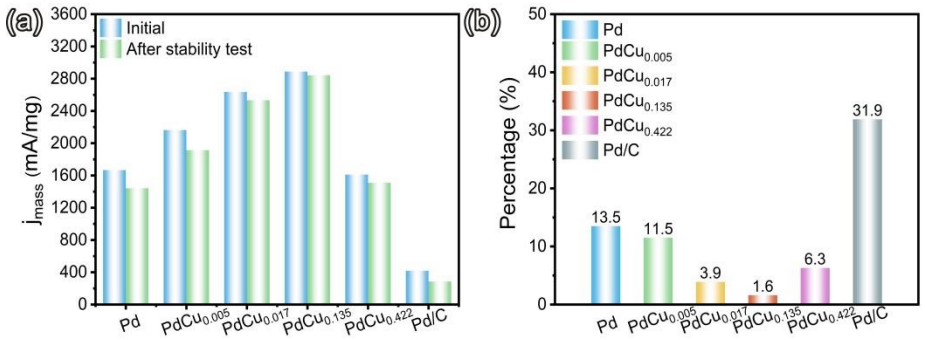

Figure S13. The MeOR stability performances of the different compositions of PdCu metallene nanocatalyst, undoped Pd metallene nanocatalyst, and commercial Pd/C catalyst before and after durability testing. (a) Mass activities. (b) The loss percentage of current density.

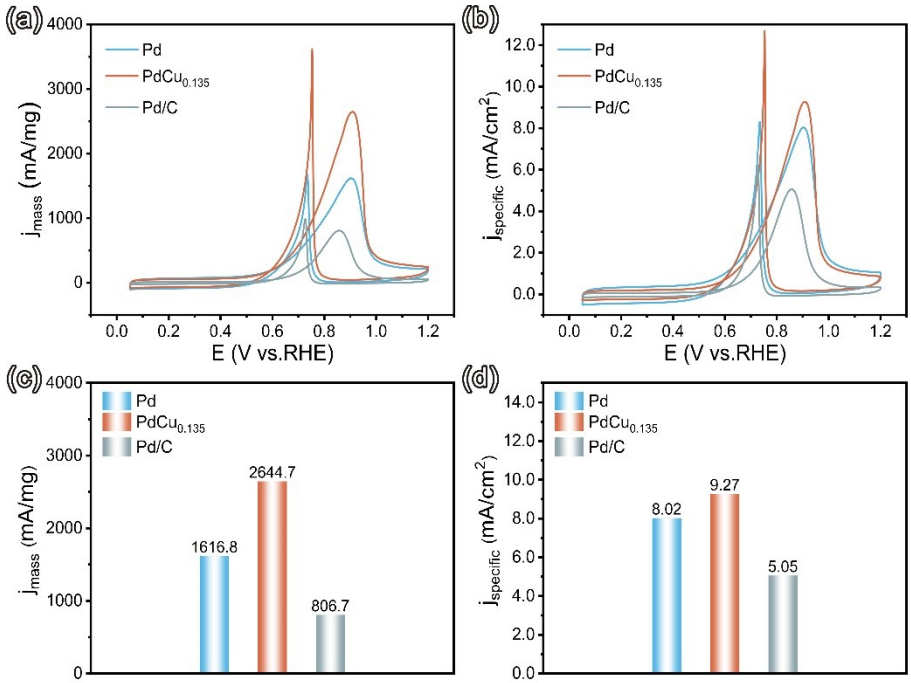

Figure S14. The EGOR performances of the commercial Pd/C, Pd Metallene, and PdCu Metallene catalysts. (a, b) Cyclic voltammetry curves in N_2-saturated EG (1 M) + KOH (1 M) solution. (c) Mass (j_{mass}) and (d) specific ($j_{specific}$) activities, the values obtained at the peak current.

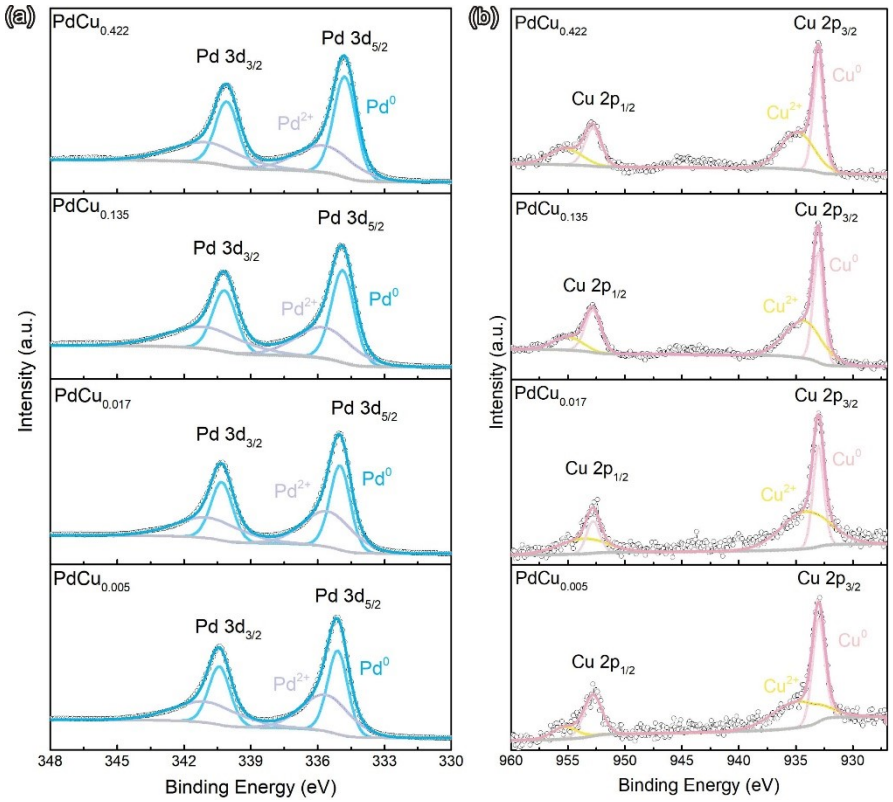

Figure S15. The XPS spectra of Pd (a) and Cu (b) elements in the PdCu metallene nanocatalyst with different compositions.

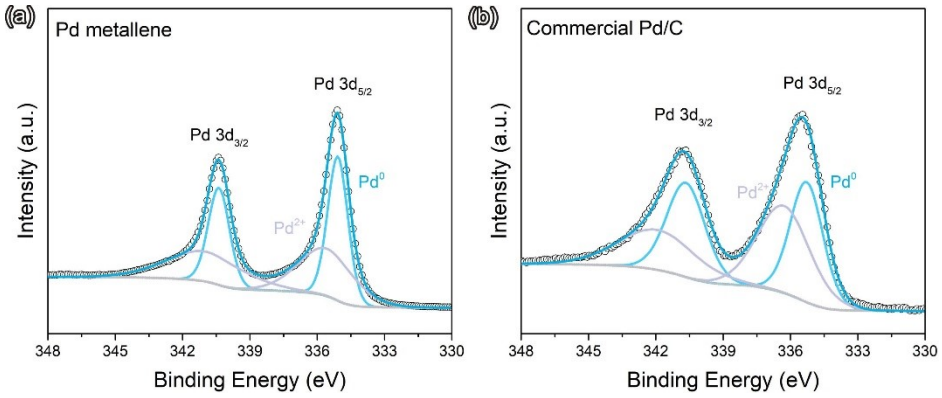

Figure S16. The XPS spectra of Pd elements in the Pd metallene nanocatalyst and commercial Pd/C catalyst.

Table S1. The metal loads of the commercial Pd/C, Pd Metallene, and PdCu Metallene catalysts with different compositions on electrode determined by ICP-MS.

Sample	Pd	$PdCu_{0.005}$	$PdCu_{0.017}$	$PdCu_{0.135}$	$PdCu_{0.422}$	Commercial Pd/C
Pd/μg	6	5.9817	5.9391	5.5457	4.7686	6
Cu/μg	0	0.0168	0.0597	0.4535	1.2302	0
Mo/μg	0	0.0015	0.0012	0.0008	0.0012	0

Table S2. The specific ECSAs of the commercial Pd/C, Pd Metallene, and PdCu Metallene catalysts with different compositions.

Catalysts	Pd	$PdCu_{0.005}$	$PdCu_{0.017}$	$PdCu_{0.135}$	$PdCu_{0.422}$	Commercial Pd/C
Specific ECSA (m^2/g)	20.14	24.25	26.69	28.53	32.45	15.95

Table S3. The EOR performances of the commercial Pd/C, Pd Metallene, and PdCu Metallene catalysts with different compositions.

Catalysts	Pd	$PdCu_{0.005}$	$PdCu_{0.017}$	$PdCu_{0.135}$	$PdCu_{0.422}$	Commercial Pd/C
J_{mass} (mA/mg_{Pd})	2600.1	3414.7	3718.2	4255.6	1963.1	746.4
$J_{specific}$ (mA/cm^2)	9.15	11.09	11.80	12.67	5.09	3.41

Table S4. The comparison of EOR performance of recently Pd-based nanocatalysts.

Catalysts	Electrolyte	J_{mass} (A/mg)	$J_{specific}$ (mA/cm^2)	References
$PdCu_{0.135}$ nanosheets	1.0 M KOH+ 1.0 M C_2H_5OH	4.26	12.67	This work
PdCoH nanosheets	1.0 M NaOH+ 1.0 M C_2H_5OH	6.26	11.0	*J. Mater. Chem. A*, 2022,10, 1735-1741
SA W−Pd metallene aerogels	1.0 M KOH+ 1.0 M C_2H_5OH	5.29	10.90	*ACS Nano*, 2022, 16, 21266–21274
MoO_x/Pd nanosheets	1.0 M KOH+ 1.0 M EtOH	3.80	8.40	*ACS Appl. Mater. Interfaces*, 2021, 13, 13311–13318
PdBi-0.5 nanocages/C	1.0 M KOH+ 1.0 M C_2H_5OH	3.49	10.37	*J. Colloid Interf. Sci.*, 2021, 591, 203–210
Pd/$NiMoO_4$−C nanorod	1.0 M KOH+ 1.0 M C_2H_5OH	3.32	-	*ACS Appl. Mater. Interfaces*, 2021, 13, 53777–53786
c-PdNiP@a-PdNiP	1.0 M KOH+ 1.0 M C_2H_5OH	3.05	11.09	*Adv. Mater.*, 2020, 32, 2000482.
PdFe nanocages	1.0 M KOH+ 1 .0 M C_2H_5OH	2.70	8.30	*Nanoscale*, 2020, 12, 2126–2132
PdCu nanosheet assemblies	1.0 M KOH+ 1.0 M C_2H_5OH	2.54	4.0	*Langmuir*, 2022, 38, 14, 4287–4294
Pd/NCB@NCNTs-2	1.0 M KOH+ 1.0 M C_2H_5OH	1.88	4.65	*Green Chem*, 2023, 25, 10033–10042
Pd-PdO_x/GS-NH_2-2	1.0 M KOH+ 1.0 M C_2H_5OH	1.32	5.30	*ACS Sustainable Chem. Eng.*, 2019, 7, 14621–14628

Table S5. The MeOR performances of the commercial Pd/C, Pd Metallene, and PdCu Metallene catalysts with different compositions.

Catalysts	Pd	$PdCu_{0.005}$	$PdCu_{0.017}$	$PdCu_{0.135}$	$PdCu_{0.422}$	Commercial Pd/C
J_{mass} (mA/mg_{Pd})	1666.7	2162.8	2635.9	2887.5	1610.4	418.5
$J_{specific}$ (mA/cm^2)	5.87	7.02	8.37	8.59	4.17	1.91

Table S6. The EGOR performances of the commercial Pd/C, Pd Metallene, and PdCu Metallene catalysts with different compositions.

Catalysts	Pd	$PdCu_{0.135}$	Commercial Pd/C
J_{mass} (mA/mg_{Pd})	1616.8	2644.7	806.7
$J_{specific}$ (mA/cm^2)	8.02	9.27	5.05